symmetry

IMPACT FACTOR 2.940

CITESCORE 4.3

Review

Review of the Applications of Kalman Filtering in Quantum Systems

Kezhao Ma, Jia Kong, Yihan Wang and Xiao-Ming Lu

Special Issue
New Frontiers in Quantum Information

Edited by
Prof. Dr. Wuming Liu and Dr. Xingdong Zhao

MDPI

https://doi.org/10.3390/sym14122478

symmetry

MDPI

Review

Review of the Applications of Kalman Filtering in Quantum Systems

Kezhao Ma, Jia Kong *, Yihan Wang and Xiao-Ming Lu *

Department of Physics, Hangzhou Dianzi University, Hangzhou 310018, China
* Correspondence: jia.kong@hdu.edu.cn (J.K.); lxm@hdu.edu.cn (X.-M.L.)

Abstract: State variable and parameter estimations are important for signal sensing and feedback control in both traditional engineering systems and quantum systems. The Kalman filter, which is one of the most popular signal recovery techniques in classical systems for decades, has now been connected to the stochastic master equations of linear quantum mechanical systems. Various studies have invested effort on mapping the state evolution of a quantum system into a set of classical filtering equations. However, establishing proper evolution models with symmetry to classical filter equation for quantum systems is not easy. Here, we review works that have successfully built a Kalman filter model for quantum systems and provide an improved method for optimal estimations. We also discuss a practical scenario involving magnetic field estimations in quantum systems, where non-linear Kalman filters could be considered an estimation solution.

Keywords: Kalman filter; stochastic master equation; stochastic filter

Citation: Ma, K.; Kong, J.; Wang, Y.; Lu, X.-M. Review of the Applications of Kalman Filtering in Quantum Systems. *Symmetry* **2022**, *14*, 2478. https://doi.org/10.3390/sym14122478

Academic Editors: Wuming Liu and Xingdong Zhao

Received: 20 October 2022
Accepted: 16 November 2022
Published: 22 November 2022

1. Introduction

Parameter estimation and real-time signal tracking methods [1] have been widely used in the engineering field [2], not only for parameter sensing and measurement [3,4], but also for feedback control systems [5,6]. With the development of quantum theory and technology, especially quantum precision measurements and quantum sensing [7], realizing parameter estimations, signal analyses and state variable control in quantum systems has become an important research topic [8–10]. Similarly to classical systems, the estimation of parameters or state variables will directly affect the feedback control of quantum systems. However, parameter and state variables estimations in quantum systems would be more complex than those in classical systems. Considering the existence of weak quantum effects and quantum fluctuations, it is a great challenge to establish a proper evolution model for state variables or parameters. Finding a suitable algorithm for data analysis and signal extraction is another difficult problem. With the development of continuous quantum measurement theory [11], researchers realized that linear quantum mechanical systems have many similarities with classical systems that are driven by specific noise. For example, in a continuously observed linear quantum system [12], the state evolution equation has symmetry to state filtering equation of a linear classical system, which is called the Kalman filtering equation [13]. Therefore, Kalman filtering methods could be introduced into quantum systems for the estimation of state variables and parameters.

The classical Kalman filter [14] has been developed for more than 50 years and is still one of the most important and common estimation algorithms. The great success of the Kalman filter is due to its small computational requirements, outstanding recursive property, and its optimal estimation method for linear systems with Gaussian error statistics [15]. The variants of the Kalman filter, such as the extended Kalman filter [16] and unscented Kalman filter [17], are extended to solve the problem of estimating the state and parameters in nonlinear systems. The Kalman filter has been applied in many areas, including navigation positioning systems [18], feedback control systems [19] and also newly developing

areas, such as machine learning [20]. The Kalman filter is also expected to provide the optimal estimation of the state variable and parameters of quantum systems [21].

In what follows, we shall mainly review how a quantum system could use the Kalman filter method for state variables or parameter estimations and the specific applications of Kalman filtering in quantum systems.

2. Realization of Kalman Filtering in Quantum Systems

In classical systems, according to Bayes statistical inferences [22,23], the best estimator $\hat{X}$ of a state variable X is the mean of the conditional probability distribution based on an observation, Z. If the state variable X is time-dependent, we hope to find the time evolution equation of the conditional probability, such as the Kushner–Stratonovich equation [24]. By properly constraining the Kushner–Stratonovich equation, we obtain the Kalman filtering equation for estimating the state variables.

Similarly to the evolution of conditional probabilities in classical systems, in quantum systems, we can derive the evolution of a "conditional quantum state" based on observations and obtain the optimal estimation of state variables. The theory of quantum continuous measurement [25] provides a solution to this problem. The state evolution of a quantum system under continuous measurements could be described by the following stochastic master equation (SME) [12]:

$$d\rho_c = -\frac{i}{\hbar}[H, \rho_c]dt + \mathcal{D}[c]\rho_c dt + \mathcal{H}[c]\rho_c dw, \tag{1}$$

where ρ_c is the quantum state conditioned on measurement outcomes, c is an operator determined by the measuring process and $\mathcal{D}[c]$ and $\mathcal{H}[c]$ are superoperators on ρ_c and will be explained in the following sections [11]. The first term on the right side of the SME represents the quantum state evolution due to the system's Hamiltonian H. The second term on the right side of the SME, which is defined as $\mathcal{D}[c]\rho_c = c\rho_c c^\dagger - \frac{1}{2}(c^\dagger c\rho_c + \rho_c c^\dagger c)$, indicates the decoherence caused by measurements. This term is similar to that for the interaction between an open quantum system [26,27] and a Markovian environment. In the third term on the right side of the SME, $\mathcal{H}[c]\rho_c = c\rho_c + \rho_c c^\dagger - \mathrm{Tr}[(c + c^\dagger)\rho_c]\rho_c$ and dw is the Wiener increment [28], which stands for a Gaussian increment introduced by continuous measurements. This term denotes the disturbance on the quantum state's evolution due to observations. The relationship between Wiener increment dw and observation increment dr is given by an observation equation [29], e.g.,

$$dw = 2dr - \langle c + c^\dagger \rangle dt \quad \text{with} \quad \langle \cdot \rangle = \mathrm{Tr}[\cdot \rho], \tag{2}$$

provided that the observable $(c + c^\dagger)/2$ is measured. We can obtain the optimal quantum state, i.e., the conditional quantum state, at each time by solving Equation (1) and then obtain the optimal estimator of any mechanical quantity by using $\mathrm{Tr}[\cdot \rho_c]$.

It is in general difficult to solve the SME. However, in some special cases, the SME can be re-arranged into a solvable form. For example, for a single quantum harmonic oscillator, the evolution equations are given by [29]

$$d\rho_c = -\frac{i}{\hbar}\left[\frac{\hat{p}^2}{2m} + \frac{1}{2}mw_0^2\hat{x}^2, \rho_c\right]dt + \mathcal{D}\left[\sqrt{2k}\hat{x}\right]\rho_c dt + \mathcal{H}\left[\sqrt{2k}\hat{x}\right]\rho_c dw, \tag{3}$$

$$dr = \sqrt{2k}\langle \hat{x} \rangle dt + \frac{dw}{2}, \tag{4}$$

where k denotes the measurement strength. If the dynamics of state variables are linear and their initial states are Gaussian, the above equations can be represented in a more intuitive form by using the canonical conjugate variables x and p satisfying the commutation relation $[\hat{x}, \hat{p}] = i\hbar$ and introducing notation $d\langle \hat{A} \rangle = \mathrm{Tr}[\hat{A}d\rho]$ ($\hat{A} = \hat{x}, \hat{p}$) as follows:

$$d\langle\hat{x}\rangle = \frac{\langle\hat{p}\rangle}{m}dt + \sqrt{8k}V_{\hat{x}}dw, \tag{5}$$

$$d\langle\hat{p}\rangle = -m\omega_0^2\langle\hat{x}\rangle dt + \sqrt{8k}C_{xp}dw, \tag{6}$$

$$\dot{V}_x = \frac{2}{m}C_{xp} - 8kV_x^2, \tag{7}$$

$$\dot{V}_p = 2\hbar^2 k - 8kC_{xp}^2 - 2m\omega_0^2 C_{xp}, \tag{8}$$

$$\dot{C}_{xp} = \frac{1}{m}V_p - 8kV_k C_{xp} - mw_0^2 V_x, \tag{9}$$

where $V_A = \langle\hat{A}^2\rangle - \langle\hat{A}\rangle^2$ is the variance, and $C_{xp} = \frac{\langle\hat{x}\hat{p}+\hat{p}\hat{x}\rangle}{2} - \langle\hat{x}\rangle\langle\hat{p}\rangle$ is the covariance. Equations (5) and (6) show the mean evolution of the position and momentum under continuous measurements. The above five equations are similar to the Kalman filter equations of the following classical system evolutions.

$$dx = \frac{p}{m}dt, \tag{10}$$

$$dp = -m\omega_0^2 x dt + \sqrt{2k}\hbar dw_c, \tag{11}$$

$$Q_c dt = 4kx dt + \sqrt{2k}dw_o. \tag{12}$$

Equation (12) is the observation equation. dw_c is the system's noise independent of the measurement noise, dw, and dw_o is the observation noise related to dw. The Kalman filter equation given by Equations (10)–(12) is actually in the same form of Equations (5)–(9), but the expectation values of operators is replaced with classical variables, and the evolution of the second moment in the SME becomes the mean square error of the estimation in the classical Kalman filter. We note that this similarity only happens if the dynamical variables are canonical coordinates that are evolving in a linear quantum system with an initial Gaussian state.

Furthermore, if we want to estimate both state variables and parameters of the system's Hamiltonian, besides the conditional quantum states evolution, we have to know the conditional probability evolution equation of parameters based on the observations. For example, to estimate parameter θ in a continuous position measurement, the system evolution could be written as [30]

$$d\rho_\theta = -i\left[\frac{\hat{x}^2}{2m} + \frac{m\omega_0^2\hat{x}^2}{2} + \theta\hat{x}, \rho_\theta\right]dt + 2k\mathcal{D}[\hat{x}]\rho_\theta dt + \sqrt{2k}\mathcal{H}[\hat{x}]\rho_\theta\left(Idt - 2\sqrt{2k}\bar{x}_\theta dt\right) \tag{13}$$

$$dp\left(\theta|I_{[0,t+dt]}\right) = 2\sqrt{2k}(\bar{x}_\theta - \bar{x})\left(Idt - 2\sqrt{2k}\bar{x}dt\right) \times P\left(\theta|I_{[0,t+dt]}\right), \tag{14}$$

where $\bar{x}_\theta$ indicates the conditional mean of the position on parameter θ, which is written as $\mathrm{Tr}[\hat{x}\rho_\theta]$. $\bar{x}$ indicates the mean of $\hat{x}$, which is written as $\mathrm{Tr}[\hat{x}\rho]$. $P\left(\theta|I_{[0,t+dt]}\right)$ is the conditional probability of θ based on the observation in time $[0, t+dt]$.

3. Applications of Kalman Filtering in Quantum Systems

In this section, we provide some examples of using Kalman filtering in quantum systems, including the position estimation and feedback control of a harmonic oscillator system [31], the estimation of magnetic fields [32], atomic spin [33] and optical field information [34] in a photon–atom interaction system, and reconstruction of quantum state in quantum tomography [35].

3.1. Position Estimation and Feedback Control

In the suspension photomechanics area, cooling and stabilizing the center of the mass' motion of a suspended nanosphere [36] are important targets that offer the possibility for measuring matter–wave interference, studying quantum effects [37], collapsing models

at smaller than atomic scales [38] and obtaining improved sensitivities compared to that of a suspended atomic system [39]. The motion of optical levitated nanospheres can be described by the motion of stochastic quantum harmonic oscillators [40]. Kalman filtering can provide the optimal estimation of the position of nano-particles; furthermore, it could apply for feedback controls. There are two common methods to realize feedback control in a dynamical system [21]. The first one uses estimation, while the other one directly uses the observation as a control term. The SME including this type of feedback Hamiltonian would still be linear and could be represented by classical Kalman filter equations.

In 2018, Setter et al. [40] used Kalman filters and FPGA (Field-Programmable Gate Array) [41] in an experiment to obtain feedback and control randomly moving nano-particles. As shown in Figure 1, the center of the mass's translation of captured nano-particles along the optical axis is cooled in three orders of magnitude from 300 K to 162 ± 15 mK. The comparison of using a band-pass filter and the Kalman filter is shown in Figure 2, where the Kalman filter significantly improves the signal estimation than other filtering methods. This work not only shows the advantages of Kalman filtering over other filtering methods, but also provides a way of applying Kalman filters in quantum fields.

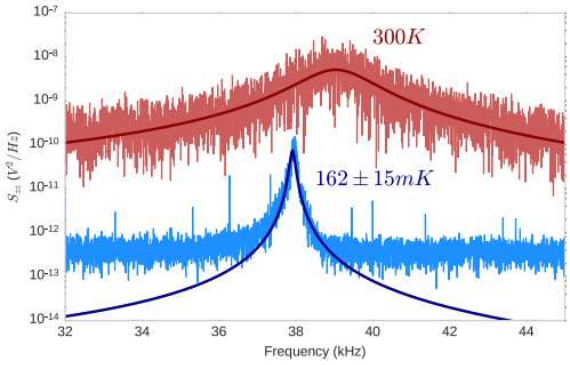

Figure 1. The power spectrum density (PSD) of uncooled particles (in red) in thermal equilibrium at 300 K (at a pressure of 3 mbar) and that of cooled particles (in blue) at a pressure of 5.7×10^{-5} mbar. The lines represent the Lorentz fit of the spectra. Figure from [40].

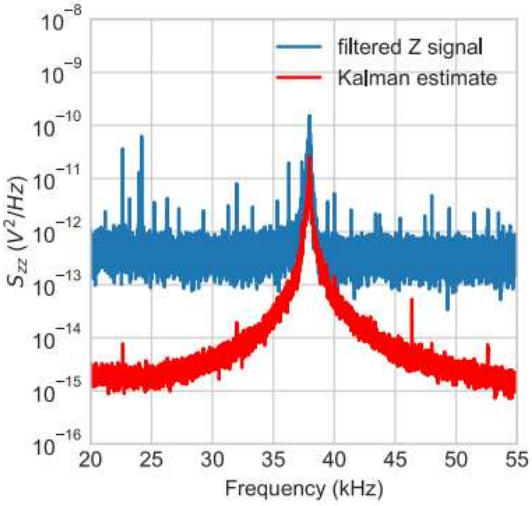

Figure 2. The comparison of Kalman filtering and band-pass filtering (filtered Z signal) results. Figure from [40].

In the experiment of cooling suspended nanoparticles, Magrini et al. [42] used Kalman filters to construct an equation for the motion of the system. They showed the verification of their Kalman filter model by demonstrating that the innovation ($\epsilon(t)$) between Kalman filter estimations ($\hat{z}(t)$) and observations ($\xi(t)$) is a Gaussian zero-mean white-noise process. The accuracy of the Kalman filtering model is verified.

JIANG et al. [43] also discussed the feasibility of applying Kalman filters to detect suspended microspheres. They showed, in Figure 3, that the root-mean-square error of the displacement of nano-spheres decreases by 1.7 nm and 3.1 nm at 101 kPa and 6 Pa, respectively, by using a Kalman filter.

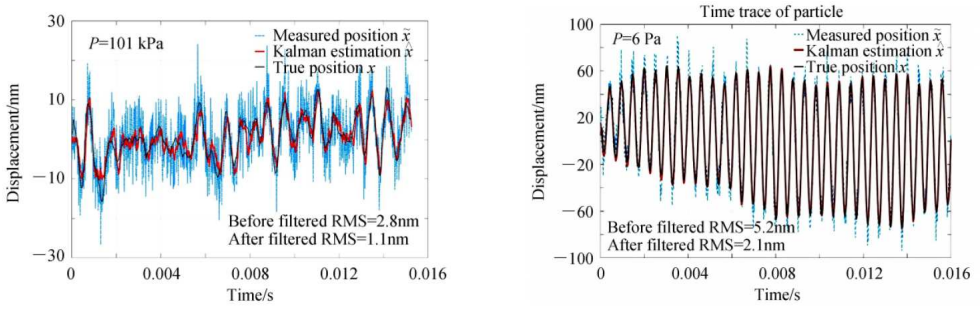

Figure 3. Time sequence of micro-particles in optical traps at 101 kPa pressure (**left**) and 6 Pa pressure (**right**), respectively. Figure from [43].

Kalman filtering is also widely used in other optical systems for variable estimation, such as optimal state estimations for cavity optomechanical systems [4], optical-phase tracking [1], external force tracking on a mirror [10], the position estimation of mirrors [21], phase and polarization estimations in quantum key distributions [44], amplitude estimations in high-speed atomic force microscopy [45], etc. [46]. These works promote the applications of Kalman filtering in quantum systems and provide ideas for extending efficient algorithms from classical engineering fields to quantum systems.

3.2. Magnetic Field Estimation

As a typical quantum sensor, atomic magnetometers [47–49] developed rapidly in the field detection area in recent years. It is one of the most sensitive magnetometers that can compete with a superconducting quantum interference device (SQUID) [50], and it can be used for brain magnetic field detection [51]. In addition, the device is compact and can work at room temperature; thus, it is also suitable for geomagnetic exploration [52], magnetic prospecting [53], submarine exploration [54], mine sweeping [55] and other fields [56]. The core design of the atomic magnetometer is based on the interaction of light and atoms. In principle, its fundamental measurement sensitivity [57,58] will be limited by optical and atomic quantum noise. At present, the method of reducing quantum noise is to combine squeezed light [59–63] or atomic spin-squeezed states [48,64,65] with an atomic magnetometer. However, it requires a substantial amount of work, such as the calibration of noise sources, understanding quantum effects and modelling system dynamics, before it can be realized. This is because, quantum squeezing is often very weak and hides below classical noise. Even after reducing most classical noise, due to quantum fluctuations, the effective information extraction is still a challenge in quantum system. Some signal extraction affected by quantum noise requires special signal recovery and data analysis methods. The conditional variance analysis method [66] is a popular solution. Kalman filtering signal recovery methods have similar ideas compared with conditional variance analyses; therefore, it has been introduced into atomic ensembles in recent years for parameter estimation and quantum noise suppression. The recovery of the magnetic field signal is hereinafter referred to as the estimation of the magnetic field's signal.

In general, an atomic magnetometer obtains signals with continuous measurements, such as the Faraday rotation measurement [67], in which the Kalman filter can play a role in state variables or system parameter estimations. However, it is not a easy task for magnetic field estimations. There are two reasons. First, the difficult stems from the observables of the atomic magnetometer system; i.e., the three components of total spin do not satisfy canonical commutation relations. To estimate both magnetic field and spin components at

the same time, the system's evolution cannot be expressed with linear dynamics. Therefore, the system's evolution cannot be expressed by a closed set of equations of low-order moments, such as $\langle J_x \rangle$, $\langle J_z \rangle$ and $\langle J_x^2 \rangle$. Second, the magnetic field is a parameter in the system's Hamiltonian. In addition to the state variable evolution model, we have to build the conditional probability evolution of the magnetic field under observation. To deal with the above problems, previous studies assumed that all atoms are polarized along one direction, and the measurement is focused on short timescales; therefore, one spin component can be treated as a constant number. Then, the system can be described by linear dynamics since the magnetic field is not coupled with any spin component. For example, if the magnetic field is applied along y direction and all atoms are polarized along the x direction, the evolution of the system can be described as follows [32,68,69]:

$$d\left\langle \hat{J}_z \right\rangle = \gamma B J e^{-Mt/2} dt + 2\sqrt{M\eta}\left\langle \Delta \hat{J}_z^2 \right\rangle dW \tag{15}$$

$$d\left\langle \hat{J}_z^2 \right\rangle = -4M\eta\left\langle \Delta \hat{J}_z^2 \right\rangle^2 dt, \tag{16}$$

where γ is the effective spin magnetic ratio, B is the magnetic field and J is the total angular momentum. M and n represent the detection intensity and detection efficiency, respectively.

The team of Geremia [32] applied Kalman filters to magnetic field estimations. They tried to find a model that can describe spin squeezing generation along the observation direction by using continuous measurements [70] and that can estimate magnetic fields beyond standard quantum limits by taking advantage of the spin-squeezed state. The SME describing the evolution of the system can be written in a relatively simple form: the first- and second-order moments of spin component's evolution.

$$d\rho_c = -i\gamma B\left[\hat{J}_y, \hat{\rho}_c\right]dt + M\mathcal{D}\left[\hat{J}_y\right]\hat{\rho}_c dt + \sqrt{M\eta}\mathcal{H}\left[\hat{J}_y\right]\hat{\rho}_c dW(t) \tag{17}$$

Kalman filtering has been used to estimate the static magnetic field in the system, and the following bounds of magnetic field estimation are obtained:

$$\delta B \approx \frac{1}{\gamma J}\sqrt{\frac{3}{M\eta t^3}}, \qquad t \gg JM^{-1}$$

where γ denotes the effective magnetogyric ratio, J denotes the total atomic spin, M and η denote the measurement intensity and efficiency, respectively, and t denotes time. Figure 4 shows the results of Kalman filtering in detail. This work gives the theoretical limit of the magnetic field measurement of an atomic magnetometer based on a very idealized model. Note that this is a very important theoretical work, even though in practice most atomic magnetometers do not satisfy the condition of great dissipation. Klaus Mølmer et al. [71,72] also discussed the mechanism of spin squeezing generated by continuous observations and provided a good theoretical contribution to the estimation of scalar magnetostatic fields and perturbation magnetic fields.

Stockton et al. [68] also considered the condition that the system has great dissipation. However, they discussed the estimation of a magnetic field that evolves with the Ornstein–Unlenbeck (OU) process [73]. In addition, they also offered a robust magnetic field estimation method by applying feedback to the system using Kalman filter techniques. In this way, the estimation remains robust even if there are unknown parameters, such as atomic density. Their model is still ideal, but it solves a very practical problem since providing accurate atomic information in an experiment is hard as it involves factors such as the atomic density, spin polarization and so on. By using the feedback technique, the magnetic field's estimation is not significantly dependent on atomic information.

Recently, Binefa and Kołodyński [69] discussed in detail the scaling of the mean square error $\Delta^2 \tilde{B}_t$ of magnetic field estimations in various cases. For example, $\Delta^2 \tilde{B}_t$ is obtained by the Classical Simulation (CS) method

$$\Delta^2\tilde{B}_t^{CS}(q_B) = \begin{cases} \frac{\gamma_y}{\gamma_g^2 t} \equiv \Delta^2\tilde{B}_t^{CS}(0), & \text{if} \quad t < \frac{1}{\gamma_g}\sqrt{\frac{\gamma_y}{q_B}}, \\ \sqrt{\frac{\gamma_y q_B}{\gamma_g^2}}, & \text{if} \quad (M+\gamma_y)^{-1} \gtrsim t > \frac{1}{\gamma_g}\sqrt{\frac{\gamma_y}{q_B}}, \end{cases} \tag{18}$$

or by the steady-state solution of the Kalman filter

$$\Delta^2\tilde{B}_t^{SS}(q_B) = \left(\frac{q_B\gamma_y}{\gamma_g^2} + \frac{1}{\gamma_g J}\sqrt{\frac{q_B^3}{M\eta}}e^{(M+\gamma_y)t/2} \right)^{1/2} \tag{19}$$

where γ_y represents the relaxation of the spin in the y direction. q_B represents the variance introduced by magnetic field noise at each time. γ_g is the effective gyromagnetic ratio. M and η are the measurement intensity and efficiency, respectively, and t is time. Figures 5 and 6 show the scaling of the magnetic field's estimation. This provides a theoretical reference for the optimal magnetic sensitivity of an atomic magnetometer.

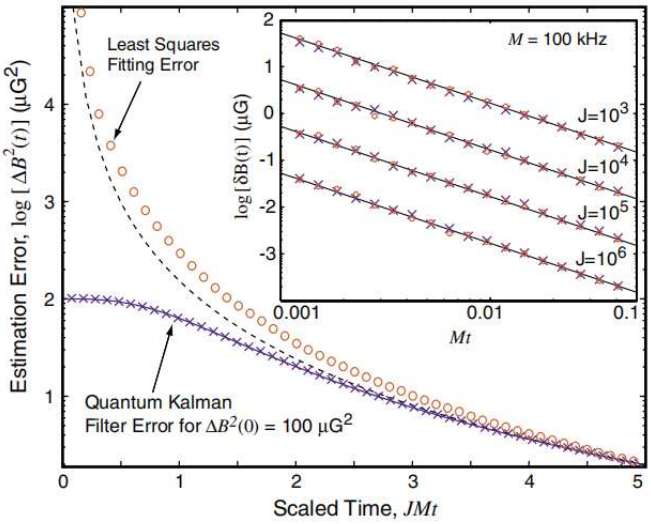

Figure 4. Comparison of the mean square error of magnetic field determination by quantum Kalman filters and linear least squares fitting. Figure from [32].

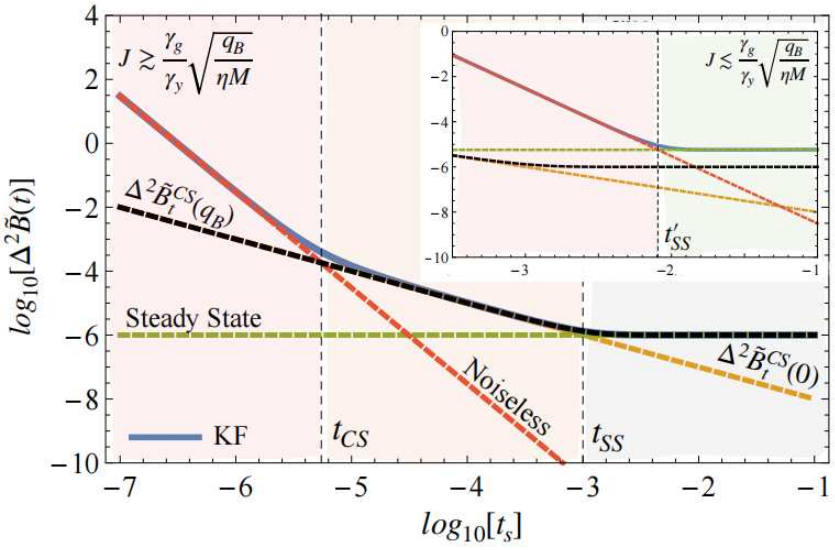

Figure 5. Mean square error of magnetic field estimations with respect to the scaled time $t_s = (M+\gamma_y)t$. The red, black, orange and green dashed lines denote the noiseless solution with $\gamma_y < M\eta$, the CS limit with $q_B > 0$, the CS limit in the absence of fluctuations ($q_B = 0$) and the steady state of the KF, respectively. Figure from [69].

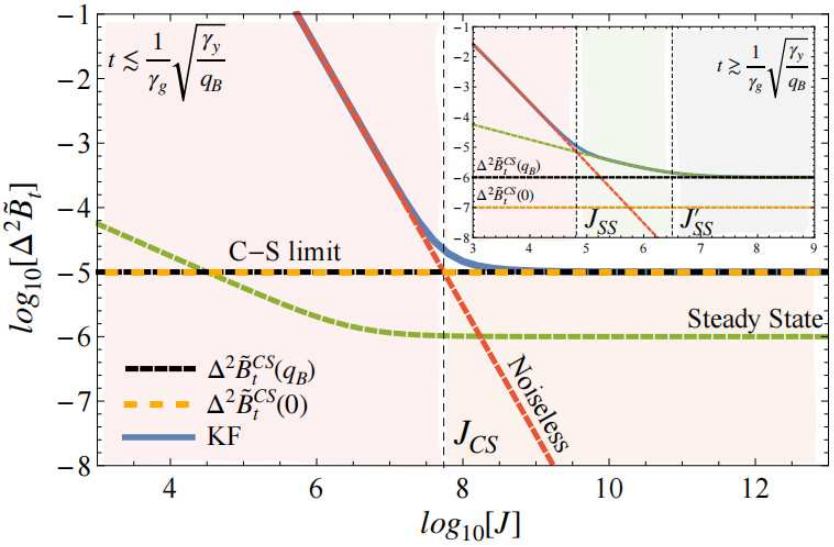

Figure 6. Mean square error of magnetic field estimations versus the size of the ensemble at $t_s = 10^{-4}$ (in the inset, $t_s = 10^{-2}$), with the same parameters as the ones used in Figure 5. Figure from [69].

Most of the above works start from the SME, and by approximation, the studies obtained a closed set of linear evolution equations for describing the quantum system's dynamics. Then, Kalman filtering was used to obtain the optimal estimation of mechanical quantities and parameters under various conditions. The purpose is to find an estimation limit that is most focused upon by theoreticians. However, experimenters tend to use Kalman filtering for data analyses to achieve better estimations and sensitivities.

3.3. Waveform Estimation and Tracking of Optical Pump

In atomic magnetometers, the angular momentum of the pump light will be transferred to spin angular momentum via resonance absorption [74], thus affecting the corresponding characteristics of the magnetic field. Therefore, the information tracking and feedback control of the pump field are also very important. The pump light, interacting with atomic spin, can be treated as a state variable or control term, and its fluctuation can be described by Gaussian white noise; therefore, it is quite reasonable to use Kalman filters for waveform tracking.

In 2018, for the first time, Martínez et al. [34] used a Kalman filter model for the waveform estimations of pump lights in an atomic magnetometer system and verified the model in an experiment. As shown in Figure 7, by comparing the known inputs of the estimated signal, the applicability of the atomic statistical model and the reliability of the Kalman filter are proved experimentally. The pump light proceeds to the Kalman filter model as a control term, as shown in the following equation:

$$dj_t = \begin{pmatrix} -\frac{1}{T_2} & \omega_l \\ -\omega_l & -\frac{1}{T_2} \end{pmatrix} j_t dt + \begin{pmatrix} 0 \\ \epsilon(t) \end{pmatrix} dt + dw_t^J, \tag{20}$$

where $j_t = [\mathrm{Tr}[j_x\rho_c], \mathrm{Tr}[j_z\rho_c]]^T$. $\epsilon(t) = g_p \cdot cos(\omega_p t) \cdot q(t) + g_p \cdot sin(\omega_p t) \cdot p(t)$ represents the waveform of the pump light. $q(t)$ and $p(t)$ are the quantities to be estimated, which are defined as follows in the OU process:

$$dq_t = -\kappa q_t dt + dw_t^q, \qquad q_t = [q_t \;\; p_t]^T, \tag{21}$$

where dw_t^J is the system noise, and its statistical characteristics are calibrated directly from experiments. Since the magnetic field is a known parameter in this model, the state variable estimation is a linear dynamical problem. Therefore, the canonical commutation relationships are not required for spin components, which means that no strict assumptions

are made in the model. This work shows that the Kalman filtering method can recover waveform details better than the sensor's intrinsic time resolution and avoid the trade-off between sensitivity and time resolution in coherent sensing. In addition, it proposes a new Kalman filter model in atomic magnetometer systems, and this has been validated by experiments for the first time. It also provides a new idea to study the factors affecting magnetic field estimations in an atomic magnetometer; in addition, it provides a model for information encryption and decryption. By using Kalman filters, information carried by pump lights can be recovered by using magnetometer systems.

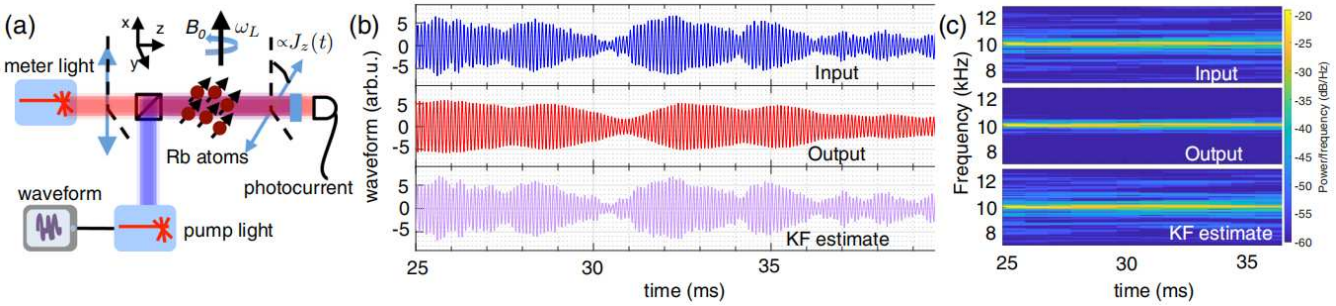

Figure 7. (**a**): Schematic diagram of atomic magnetometer. (**b**): Comparison of time trace of input signal, output signal and Kalman filter estimation. (**c**): Comparison of the power spectrum density of input signal, output signal and Kalman filtering. Figure from [34].

3.4. Estimation of Spin Components and Noise Squeezing

In the theoretical studies of magnetic field estimations [75], it has been shown that the accumulation of continuously measured information can bring spin noise squeezing so that the magnetic field estimation can reach the Heisenberg limit. However, there are many sources of noise and complex atomic collision processes in magnetic sensing devices based on thermal atomic systems, which make the preparation and detection of squeezed states extremely challenging. Kalman filters provide both the mean value and the mean square error of the state estimation based on accumulated information via measurements. This is very helpful for quantum noise analyses and noise squeezing evaluation.

In 2020, Kong et al. [33] first applied the Kalman filtering method in a spin exchange relaxation-free (SERF) atomic system for data analyses and squeezed state/entangled state detection. Under high temperatures and strong interaction conditions where the SERF atomic magnetometer [76] operates, a macroscopic entangled state with 10^{13} atoms is successfully achieved by quantum non-destructive measurements [77]. In this study, the magnetic field is treated as a known parameter, and only spin variables are estimated. This guarantees a linear dynamic model that could be applied with Kalman filter equations. The Kalman filtering method played an important role in data analyses. As shown in Figure 8, it has been used to extract spin noise components from observation signals that can compare with the entanglement criterion [78]. In this experiment, the weak polarization condition is considered. All atomic spins are initially in a thermal state. The Faraday rotation measurement method is used to prepare correlations. Under this condition, the evolution of the system can be written in the following way:

$$d\mathcal{F} = -A\mathcal{F}dt + \sqrt{\sigma}dW,$$

where the matrix element of operator A is $A_{ij} = -\gamma B_h \epsilon_{hij} + \Gamma_{ij}$,$h, i, j = x, y, z$, Γ_{ij} denotes system relaxation, B_h is the magnetic field and $\sqrt{\sigma}dW$ is the intrinsic spin noise.

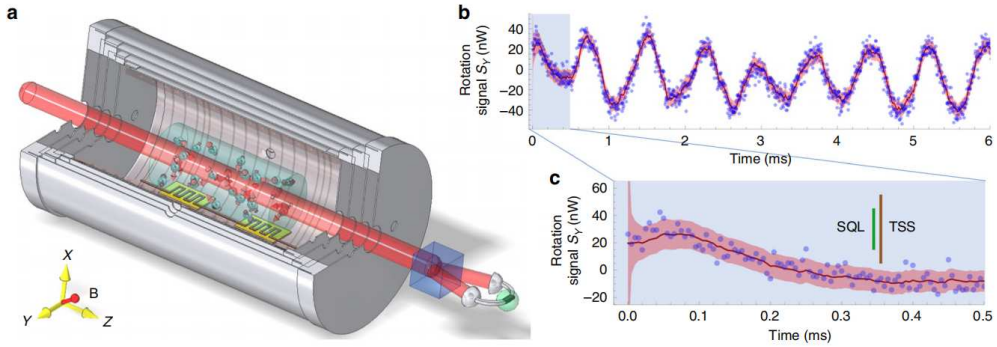

Figure 8. (**a**): Experimental setup diagram. (**b**): Klaman filter estimation of the Stocks parameter S_y with the mean value (red line) and mean square error (pink shadow) based on experimental data (blue dot) and the optimal estimation for the atomic spin, $g\mathcal{F}S_x$ (red line). (**c**): Zoomed-in view the early signal. Figure from [33].

In this study, the Monte Carlo simulation method [79] has been used to conduct a series of comparisons between the theory and experiment to validate the Kalman filtering model. The largest macroscopic entangled state at present, macroscopic spin singlet state [80], is successfully observed. This is also the first time quantum effects were observed under the SERF mechanism, which opens a new platform for quantum optics research and encourages the study of quantum-enhanced precision measurements in high-temperature thermal atomic systems. This work further expands the application scope of Kalman filters in a quantum system and applies Kalman filters for noise estimation and data analysis.

3.5. Density Matrix Estimation in Quantum Tomography

Filtration procedures can also help for density matrix estimations [81], for example, Kalman filter has been used for static quantum state estimation (reconstruction) in quantum tomography [35,82–85]. Quantum state tomography reconstructs quantum states from experimental data [35], which are mapped onto quantum states by a set of measurement operators. Because of intuitiveness, it is useful for correlation or entanglement quantifications [86]. Different than common dynamical state estimation, in quantum tomography, so far only Kalman filter update equations are used for quantum state reconstruction [35]. This is because the system has to be static in quantum tomography.

In 2009, Audenaert et al. [35] applied the Kalman filter method for errorbar estimation of a quantum state measurement with few discrete outcomes, which corresponds to a probability density function (PDF) over state space. By simplifying the Bayes statistical inference equation, they obtain the following Kalman filtering update equations [35]:

$$\tilde{K} = \tilde{\Sigma}\tilde{H}^T\left(\tilde{H}\tilde{\Sigma}\tilde{H}^T + \tilde{\Theta}\right)^{-1}, \tag{22}$$

$$\tilde{\mu}^{'} = \tilde{\mu} + \tilde{K}\left(\tilde{z} - \tilde{H}\tilde{\mu}\right), \tag{23}$$

$$\tilde{\Sigma}^{'} = \tilde{\Sigma} - \tilde{K}\tilde{H}\tilde{\Sigma}, \tag{24}$$

where $\tilde{\mu}$ is the estimated value, $\tilde{\Sigma}$ is the covariance of estimated value, $\tilde{H}$ represents measurement matrix, $\tilde{z}$ and $\tilde{\Theta}$ are related to the mean and variance of the posterior distribution, respectively. Using the covariance calculated by the above equations, errorbar of derived quantities can be easily calculated. They also showed two practical applications of this method: the state reconstruction of an entangled two-qubit state, and reconstruction of an optical positive operator value measure (POVM).

In the analysis of Czerwinski [86], the Kalman filter method has also been compared with other density matrix reconstruction methods, such as least-squares reconstruction and maximum likelihood reconstruction. They pointed out that Kalman filter outperforms the other reconstruction methods with the standard formula for the expected counts. However,

the Kalman filter has inferior results in entanglement quantification when the standard approach involves a linear model of dark counts [86].

Furthermore, if the processes are not linear or the initial system is not Gaussian, such as Fock or cat states, linear Kalman filters can not provide an optimal estimation. Therefore, nonlinear Kalman filters or other filter methods, such as Stratonovich's filtering theory [87] and the tomographic filtering method [88], have been studied for obtaining optimal estimations in quantum systems.

4. Conclusions and Discussion

Here, we discuss the connection of the classical Kalman filter method [13] and continuous quantum measurement theory [29] and how to derive Kalman filter equations from the SME of a quantum system. We also reviewed the successful applications of Kalman filters in quantum systems, including the position estimation of harmonic oscillator systems [40] and magnetic field estimations [32], spin component estimations [33] and tracking the pump light's waveform in an atomic magnetometer system [34], and also the reconstruction of quantum state in quantum tomography [35]. In these linear or nearly linear systems with Gaussian noise, Kalman filtering is an better method for optimal estimation. It offers easier solutions for quantum estimations and also allows engineers to contribute to quantum physics quickly. However, nonlinear models often appear in practice where linear Kalman filters are not applicable. This is a major limitation for its applications.

In a system with light, atom and magnetic field interactions, there are still many challenging problems, such as choosing the appropriate model for the system and the Kalman filtering method for a nonlinear evolution process. Currently, all theoretical studies for magnetic field estimations using the Kalman filter method assume that the evolution of a system has large dissipations. In the assumption, atomic spins satisfy the canonical commutation relationship; thus, it can make an optimal estimation relative to the magnetic field with the linear Kalman filter equation. For magnetic field estimations in a more practical highly sensitive atomic magnetometer system in which the large dissipation assumption may not valid, the state variable evolution contains the quadratic term for the spin and magnetic field's coupling. The next step could be to use nonlinear Kalman filtering methods, such as extended Kalman filtering [16] and unscented Kalman filtering [89], to build a more general model for atomic magnetometers. We note that the extended Kalman filter can only be numerically solved. Therefore, it cannot produce the optimal estimation, but it provides a reference for finding the optimal method for magnetic field estimations relative to general atomic magnetometers.

Author Contributions: Conceptualization, J.K. and K.M.; literature research, K.M., J.K. and Y.W.; original draft preparation, K.M.; review and editing, J.K., X.-M.L. and Y.W.; supervision, J.K.; project administration, J.K. and X.-M.L.; funding acquisition, J.K. and X.-M.L. All authors have read and agreed to the published version of the manuscript.

Funding: This research was supported from the National Natural Science Foundation of China (NSFC) (Grant No. 12005049, No. 11935012, No. 61871162 and No. 12275062).

Institutional Review Board Statement: Not applicable.

Informed Consent Statement: Not applicable.

Data Availability Statement: Not applicable.

Conflicts of Interest: The authors declare no conflict of interest.

References

1. Yonezawa, H.; Nakane, D.; Wheatley, T.A.; Iwasawa, K.; Takeda, S.; Arao, H.; Ohki, K.; Tsumura, K.; Berry, D.W.; Ralph, T.C.; et al. Quantum-Enhanced Optical-Phase Tracking. *Science* **2012**, *337*, 1514–1517. [CrossRef] [PubMed]
2. Korayem, A.H.; Khajepour, A.; Fidan, B. A Review on Vehicle-Trailer State and Parameter Estimation. *IEEE Trans. Intell. Transp. Syst.* **2021**, *23*, 5993–6010. [CrossRef]
3. Kitching, J.; Knappe, S.; Donley, E.A. Atomic Sensors—A Review. *IEEE Sens. J.* **2011**, *11*, 1749–1758. [CrossRef]

4. Wieczorek, W.; Hofer, S.G.; Hoelscher-Obermaier, J.; Riedinger, R.; Hammerer, K.; Aspelmeyer, M. Optimal State Estimation for Cavity Optomechanical Systems. *Phys. Rev. Lett.* **2015**, *114*, 223601. [CrossRef]
5. Rossi, M.; Mason, D.; Chen, J.; Tsaturyan, Y.; Schliesser, A. Measurement-based quantum control of mechanical motion. *Nature* **2018**, *563*, 53–58. [CrossRef]
6. Geremia, J.M.; Stockton, J.K.; Mabuchi, H. Real-Time Quantum Feedback Control of Atomic Spin-Squeezing. *Science* **2004**, *304*, 270–273. [CrossRef]
7. Degen, C.L.; Reinhard, F.; Cappellaro, P. Quantum sensing. *Rev. Mod. Phys.* **2017**, *89*, 035002. [CrossRef]
8. Tsang, M.; Wiseman, H.M.; Caves, C.M. Fundamental Quantum Limit to Waveform Estimation. *Phys. Rev. Lett.* **2011**, *106*, 090401. [CrossRef]
9. Tsang, M. Optimal waveform estimation for classical and quantum systems via time-symmetric smoothing. *Phys. Rev. A* **2009**, *80*, 033840. [CrossRef]
10. Iwasawa, K.; Makino, K.; Yonezawa, H.; Tsang, M.; Davidovic, A.; Huntington, E.; Furusawa, A. Quantum-Limited Mirror-Motion Estimation. *Phys. Rev. Lett.* **2013**, *111*, 163602. [CrossRef] [PubMed]
11. Wiseman, H.M.; Milburn, G.J. *Quantum Measurement and Control*; Cambridge University Press: Cambridge, MA, USA, 2010.
12. Jacobs, K. *Quantum Measurement Theory and Its Applications*; Cambridge University Press: Cambridge, MA, USA, 2014.
13. Kalman, R. A New Approach to Linear Filtering and Prediction Problems. *J. Basic Eng.* **1960**, *82D*, 35–45. [CrossRef]
14. Kalman, R.; Bucy, R. New Results in Linear Filtering and Prediction Theory. *ASME J. Basic Eng. Ser. D* **1973**, *83*, 95–108. [CrossRef]
15. Jacobs, K. *Stochastic Processes for Physicists Understanding Noisy Systems*; Cambridge University Press: Cambridge, MA, USA, 2010.
16. Costa, P.J. Adaptive model architecture and extended Kalman-Bucy filters. *IEEE Trans. Aerosp. Electron. Syst.* **1994**, *30*, 525–533. [CrossRef]
17. Julier, S.J.; Uhlmann, J.K. Unscented filtering and nonlinear estimation. *Proc. IEEE* **2004**, *92*, 401–422. [CrossRef]
18. Cooper, S.; Durrant-Whyte, H. A Kalman filter model for GPS navigation of land vehicles. In Proceedings of the IEEE/RSJ International Conference on Intelligent Robots and Systems (IROS'94), Munich, Germany, 12–16 September 1994; Volume 1, pp. 157–163. [CrossRef]
19. Auger, F.; Hilairet, M.; Guerrero, J.M.; Monmasson, E.; Orlowska-Kowalska, T.; Katsura, S. Industrial Applications of the Kalman Filter: A Review. *IEEE Trans. Ind. Electron.* **2013**, *60*, 5458–5471. [CrossRef]
20. Carron, A.; Todescato, M.; Carli, R.; Schenato, L.; Pillonetto, G. Machine learning meets Kalman Filtering. In Proceedings of the 2016 IEEE 55th Conference on Decision and Control (CDC), Las Vegas, NV, USA, 12–14 December 2016; pp. 4594–4599. [CrossRef]
21. Doherty, A.C.; Jacobs, K. Feedback control of quantum systems using continuous state estimation. *Phys. Rev. A* **1999**, *60*, 2700–2711. [CrossRef]
22. Brettorst, G.L. *Bayesian Spectrum Analysis and Parameter Estimation*; Springer: Berlin/Heidelberg, Germany, 1988.
23. van Trees, H.L.; Bell, K.L.; Tian, Z. *Detection, Estimation, and Modulation Theory. Part I: Detection, Estimation and Filtering Theory*; Wiley: New York, NY, USA, 2013.
24. Bain, A.; Crisan, D. *Fundamentals of Stochastic Filtering*; Springer: Berlin/Heidelberg, Germany, 2008.
25. Caves, C.M.; Milburn, G.J. Quantum-mechanical model for continuous position measurements. *Phys. Rev. A* **1987**, *36*, 5543–5555. [CrossRef] [PubMed]
26. Czerwinski, A. Dynamics of Open Quantum Systems—Markovian Semigroups and Beyond. *Symmetry* **2022**, *14*, 1752. [CrossRef]
27. Czerwinski, A. Entanglement Dynamics Governed by Time-Dependent Quantum Generators. *Axioms* **2022**, *11*, 589. [CrossRef]
28. Wiener, N. *Extrapolation, Interpolation, and Smoothing of Stationary Time Series: With Engineering Applications*; The MIT Press: Cambridge, MA, USA, 1949.
29. Jacobs, K.; Steck, D.A. A straightforward introduction to continuous quantum measurement. *Contemp. Phys.* **2006**, *47*, 279–303. [CrossRef]
30. Verstraete, F.; Doherty, A.C.; Mabuchi, H. Sensitivity optimization in quantum parameter estimation. *Phys. Rev. A* **2001**, *64*, 032111. [CrossRef]
31. Doherty, A.C.; Tan, S.M.; Parkins, A.S.; Walls, D.F. State determination in continuous measurement. *Phys. Rev. A* **1999**, *60*, 2380–2392. [CrossRef]
32. Geremia, J.M.; Stockton, J.K.; Doherty, A.C.; Mabuchi, H. Quantum Kalman Filtering and the Heisenberg Limit in Atomic Magnetometry. *Phys. Rev. Lett.* **2003**, *91*, 250801. [CrossRef] [PubMed]
33. Kong, J.; Jiménez-Martínez, R.; Troullinou, C.; Lucivero, V.G.; Tóth, G.; Mitchell, M.W. Measurement-induced, spatially-extended entanglement in a hot, strongly-interacting atomic system. *Nat. Commun.* **2020**, *11*, 2415. [CrossRef]
34. Jiménez-Martínez, R.; Kołodyński, J.; Troullinou, C.; Lucivero, V.G.; Kong, J.; Mitchell, M.W. Signal Tracking Beyond the Time Resolution of an Atomic Sensor by Kalman Filtering. *Phys. Rev. Lett.* **2018**, *120*, 040503. [CrossRef] [PubMed]
35. Audenaert, K.M.R.; Scheel, S. Quantum tomographic reconstruction with error bars: A Kalman filter approach. *New J. Phys.* **2009**, *11*, 023028. [CrossRef]
36. Aspelmeyer, M.; Kippenberg, T.J.; Marquardt, F. Cavity optomechanics. *Rev. Mod. Phys.* **2014**, *86*, 1391–1452. [CrossRef]
37. Hornberger, K.; Gerlich, S.; Haslinger, P.; Nimmrichter, S.; Arndt, M. Colloquium: Quantum interference of clusters and molecules. *Rev. Mod. Phys.* **2012**, *84*, 157–173. [CrossRef]

38. Bera, S.; Motwani, B.; Singh, T.P.; Ulbricht, H. A proposal for the experimental detection of CSL induced random walk. *Sci. Rep.* **2015**, *5*, 7664. [CrossRef]
39. Jain, V.; Gieseler, J.; Moritz, C.; Dellago, C.; Quidant, R.; Novotny, L. Direct Measurement of Photon Recoil from a Levitated Nanoparticle. *Phys. Rev. Lett.* **2016**, *116*, 243601. [CrossRef]
40. Setter, A.; Toroš, M.; Ralph, J.F.; Ulbricht, H. Real-time Kalman filter: Cooling of an optically levitated nanoparticle. *Phys. Rev. A* **2018**, *97*, 033822. [CrossRef]
41. Monmasson, E.; Cirstea, M.N. FPGA Design Methodology for Industrial Control Systems—A Review. *IEEE Trans. Ind. Electron.* **2007**, *54*, 1824–1842. [CrossRef]
42. Magrini, L.; Rosenzweig, P.; Bach, C.; Deutschmann-Olek, A.; Hofer, S.G.; Hong, S.; Kiesel, N.; Kugi, A.; Aspelmeyer, M. Real-time optimal quantum control of mechanical motion at room temperature. *Nature* **2021**, *595*, 373–377. [CrossRef] [PubMed]
43. Jiang, J.; Hu, H.; Li, N.; Chen, X.; Shu, X.; Liu, C.; Fu, Z.; Gao, X. Displacement of Optically Trapped Microsphere in Vacuum Based on Kalman Filter. *Acta Photonica Sin.* **2020**, *49*, 0512004. [CrossRef]
44. Wang, T.; Huang, P.; Wang, S.; Zeng, G. Polarization-state tracking based on Kalman filter in continuous-variable quantum key distribution. *Opt. Express* **2019**, *27*, 26689–26700. [CrossRef]
45. Ruppert, M.G.; Karvinen, K.S.; Wiggins, S.L.; Moheimani, S.O.R. A Kalman Filter for Amplitude Estimation in High-Speed Dynamic Mode Atomic Force Microscopy. *IEEE Trans. Control Syst. Technol.* **2016**, *24*, 276–284. [CrossRef]
46. Cheiney, P.; Fouché, L.; Templier, S.; Napolitano, F.; Battelier, B.; Bouyer, P.; Barrett, B. Navigation-Compatible Hybrid Quantum Accelerometer Using a Kalman Filter. *Phys. Rev. Appl.* **2018**, *10*, 034030. [CrossRef]
47. Budker, D.; Romalis, M. Optical magnetometry. *Nat. Phys.* **2007**, *3*, 227–234. [CrossRef]
48. Colangelo, G.; Ciurana, F.M.; Bianchet, L.C.; Sewell, R.J.; Mitchell, M.W. Simultaneous tracking of spin angle and amplitude beyond classical limits. *Nature* **2017**, *543*, 525–528. [CrossRef] [PubMed]
49. Kominis, I.K.; Kornack, T.W.; Allred, J.C.; Romalis, M.V. A subfemtotesla multichannel atomic magnetometer. *Nature* **2003**, *422*, 596–599. [CrossRef]
50. Tralshawala, N.; Claycomb, J.R.; Miller, J.H. Practical SQUID instrument for non-destructive testing. *Appl. Phys. Lett* **1997**, *71*, 1573. [CrossRef]
51. Xia, H.; Baranga, A.B.; Hoffman, D.; Romalis, M.V. Magnetoencephalography with an atomic magnetometer. *Appl. Phys. Lett.* **2006**, *89*, 211104. [CrossRef]
52. Xu, S.; Crawford, C.W.; Rochester, S.; Yashchuk, V.; Budker, D.; Pines, A. Submillimeter-resolution magnetic resonance imaging at the Earth's magnetic field with an atomic magnetometer. *Phys. Rev. A* **2008**, *78*, 013404. [CrossRef]
53. Alexandrov, E.B. Recent Progress in Optically Pumped Magnetometers. *Phys. Scr.* **2003**, *2003*, 27. [CrossRef]
54. Sutton, G.J.; Bitmead, R.R. Experiences with model predictive control applied to a nonlinear constrained submarine. In Proceedings of the 37th IEEE Conference on Decision and Control (Cat. No.98CH36171), Tampa, FL, USA, 18 December 1998; Volume 2, pp. 1370–1375. [CrossRef]
55. Miller, J.B. Chapter 7—Nuclear Quadrupole Resonance Detection of Explosives. In *Counterterrorist Detection Techniques of Explosives*; Yinon, J., Ed.; Elsevier Science B.V.: Amsterdam, The Netherlands, 2007; pp. 157–198.
56. Bison, G.; Wynands, R.; Weis, A. A laser-pumped magnetometer for the mapping of human cardiomagnetic fields. *Appl. Phys. B* **2003**, *76*, 325–328. [CrossRef]
57. Auzinsh, M.; Budker, D.; Kimball, D.F.; Rochester, S.M.; Stalnaker, J.E.; Sushkov, A.O.; Yashchuk, V.V. Can a Quantum Nondemolition Measurement Improve the Sensitivity of an Atomic Magnetometer? *Phys. Rev. Lett.* **2004**, *93*, 173002. [CrossRef]
58. Novikova, I.; Mikhailov, E.E.; Xiao, Y. Excess optical quantum noise in atomic sensors. *Phys. Rev. A* **2015**, *91*, 051804. [CrossRef]
59. Troullinou, C.; Jiménez-Martínez, R.; Kong, J.; Lucivero, V.G.; Mitchell, M.W. Squeezed-Light Enhancement and Backaction Evasion in a High Sensitivity Optically Pumped Magnetometer. *Phys. Rev. Lett.* **2021**, *127*, 193601. [CrossRef]
60. Wolfgramm, F.; Cerè, A.; Beduini, F.A.; Predojević, A.; Koschorreck, M.; Mitchell, M.W. Squeezed-Light Optical Magnetometry. *Phys. Rev. Lett.* **2010**, *105*, 053601. [CrossRef]
61. Horrom, T.; Singh, R.; Dowling, J.P.; Mikhailov, E.E. Quantum-enhanced magnetometer with low-frequency squeezing. *Phys. Rev. A* **2012**, *86*, 023803. [CrossRef]
62. Otterstrom, N.; Pooser, R.C.; Lawrie, B.J. Nonlinear optical magnetometry with accessible in situ optical squeezing. *Opt. Lett.* **2014**, *39*, 6533–6536. [CrossRef] [PubMed]
63. Zhang, C.; Mølmer, K. Estimating a fluctuating magnetic field with a continuously monitored atomic ensemble. *Phys. Rev. A* **2020**, *102*, 063716. [CrossRef]
64. Bao, H.; Duan, J.; Jin, S.; Lu, X.; Li, P.; Qu, W.; Wang, M.; Novikova, I.; Mikhailov, E.E.; Zhao, K.F.; et al. Spin squeezing of 10^{11} atoms by prediction and retrodiction measurements. *Nature* **2020**, *581*, 159–163. [CrossRef] [PubMed]
65. Shah, V.; Vasilakis, G.; Romalis, M.V. High Bandwidth Atomic Magnetometery with Continuous Quantum Nondemolition Measurements. *Phys. Rev. Lett.* **2010**, *104*, 013601. [CrossRef]
66. Behbood, N.; Martin Ciurana, F.; Colangelo, G.; Napolitano, M.; Tóth, G.; Sewell, R.J.; Mitchell, M.W. Generation of Macroscopic Singlet States in a Cold Atomic Ensemble. *Phys. Rev. Lett.* **2014**, *113*, 093601. [CrossRef]
67. Isayama, T.; Takahashi, Y.; Tanaka, N.; Toyoda, K.; Ishikawa, K.; Yabuzaki, T. Observation of Larmor spin precession of laser-cooled Rb atoms via paramagnetic Faraday rotation. *Phys. Rev. A* **1999**, *59*, 4836–4839. [CrossRef]

68. Stockton, J.K.; Geremia, J.M.; Doherty, A.C.; Mabuchi, H. Robust quantum parameter estimation: Coherent magnetometry with feedback. *Phys. Rev. A* **2004**, *69*, 032109. [CrossRef]
69. Amorós-Binefa, J.; Kołodyński, J. Noisy atomic magnetometry in real time. *New J. Phys.* **2021**, *23*, 123030. [CrossRef]
70. Kuzmich, A.; Mandel, L.; Bigelow, N.P. Generation of Spin Squeezing via Continuous Quantum Nondemolition Measurement. *Phys. Rev. Lett.* **2000**, *85*, 1594–1597. [CrossRef]
71. Mølmer, K.; Madsen, L.B. Estimation of a classical parameter with Gaussian probes: Magnetometry with collective atomic spins. *Phys. Rev. A* **2004**, *70*, 052102. [CrossRef]
72. Petersen, V.; Mølmer, K. Estimation of fluctuating magnetic fields by an atomic magnetometer. *Phys. Rev. A* **2006**, *74*, 043802. [CrossRef]
73. Gardiner, C.W. *Handbook of Stochastic Methods*; Springer: Berlin/Heidelberg, Germany, 1985.
74. Budker, D.; Gawlik, W.; Kimball, D.F.; Rochester, S.M.; Yashchuk, V.V.; Weis, A. Resonant nonlinear magneto-optical effects in atoms. *Rev. Mod. Phys.* **2002**, *74*, 1153–1201. [CrossRef]
75. Albarelli, F.; Rossi, M.A.C.; Paris, M.G.A.; Genoni, M.G. Ultimate limits for quantum magnetometry via time-continuous measurements. *New J. Phys.* **2017**, *19*, 123011. [CrossRef]
76. Dang, H.B.; Maloof, A.C. Ultrahigh sensitivity magnetic field and magnetization measurements with an atomic magnetometer. *Appl. Phys. Lett.* **2010**, *97*, 151110. [CrossRef]
77. Grangier, P.; Levenson, J.A.; Poizat, J.P. Quantum non-demolition measurements in optics. *Nature* **1998**, *396*, 537–542. [CrossRef]
78. Vitagliano, G.; Hyllus, P.; Egusquiza, I.L.; Tóth, G. Spin Squeezing Inequalities for Arbitrary Spin. *Phys. Rev. Lett.* **2011**, *107*, 240502. [CrossRef]
79. Mooney, C.Z. *Monte Carlo Simulation*; Sage Publications, Inc.: New York, NY, USA, 1997.
80. Tóth, G.; Mitchell, M.W. Generation of macroscopic singlet states in atomic ensembles. *New J. Phys.* **2010**, *12*, 053007. [CrossRef]
81. Warszawski, P.; Wiseman, H.M.; Doherty, A.C. Solving quantum trajectories for systems with linear Heisenberg-picture dynamics and Gaussian measurement noise. *Phys. Rev. A* **2020**, *102*, 042210. [CrossRef]
82. Czerwinski, A.; Szlachetka, J. Efficiency of photonic state tomography affected by fiber attenuation. *Phys. Rev. A* **2022**, *105*, 062437. [CrossRef]
83. Czerwinski, A.; Czerwinski, K. Statistical Analysis of the Photon Loss in Fiber-Optic Communication. *Photonics* **2022**, *9*, 568. [CrossRef]
84. Horn, R.T.; Kolenderski, P.; Kang, D.; Abolghasem, P.; Scarcella, C.; Frera, A.D.; Tosi, A.; Helt, L.G.; Zhukovsky, S.V.; Sipe, J.E.; et al. Inherent polarization entanglement generated from a monolithic semiconductor chip. *Sci. Rep.* **2013**, *3*, 2314. [CrossRef] [PubMed]
85. Czerwinski, A. Selected Concepts of Quantum State Tomography. *Optics* **2022**, *3*, 268–286. [CrossRef]
86. Czerwinski, A. Entanglement quantification enhanced by dark count correction. *Int. J. Quantum Inf.* **2022**, *20*, 2250021. [CrossRef]
87. Man'Ko, V.; Markovich, L. Optimal Nonlinear Filtering of Quantum State. *IEEE Trans. Inf. Theory* **2017**, *64*, 4784–4791.[CrossRef]
88. Aguirre, C.; Mendes, R.V. Signal recognition and adapted filtering by non-commutative tomography. *IET Signal Process.* **2014**, *8*, 67–75. [CrossRef]
89. Wan, E.A.; Van Der Merwe, R. The unscented Kalman filter for nonlinear estimation. In Proceedings of the IEEE 2000 Adaptive Systems for Signal Processing, Communications, and Control Symposium, Lake Louise, AB, Canada, 1–4 October 2000; pp. 153–158. [CrossRef]